Progress In Electromagnetics Research, PIER 17, 305–321, 1997

AN EFFECTIVE HYBRID METHOD FOR ELECTROMAGNETIC SCATTERING FROM INHOMOGENEOUS OBJECTS

Z. Xiang and Y. Lu

School of Electrical and Electronic Engineering,
Nanyang Technological University
Nanyang Avenue, Singapore 639798

1. INTRODUCTION

The problems of electromagnetic (EM) scattering and absorption by inhomogeneous, lossy, and arbitrarily shaped scatterers have been extensively dealt with in the literature because such kinds of models can simulate many practical situations including the scattering from flight objects with coated complex materials, the coupling to missiles with dielectric-filled apertures, and the performance of communication antennas in the presence of electric and magnetic inhomogeneities, etc.

Several well-known numerical techniques have been developed to solve subclasses of such kinds of EM problems. Among them are the MoM solutions [1] using either surface integral [2] or volume integral equations [3], the unimoment method [4], the FEM [5], and so on [6]. Recently, some hybrid techniques [7–11], generally consisting of two groups of techniques, have been developed for a wide range of EM

problems. These hybrid methods use a finite method such as the FEM to treat the bounded, inhomogeneous region and an integral equation method to handle the unbounded homogeneous region. Although the FEM requires less CPU time and memory due to its resultant sparse matrix, the use of traditional basis and weighting functions in the MoM always results in a full matrix equation. For large-size EM problems the cost to directly solve the dense matrix equation is very expensive and formidable.

Recently, wavelets [12–15] have been widely studied and applied by researchers in various engineering areas. Their applications in electromagnetics are getting increasing attention [16–18]. More recently, the wavelet transform has been extended in the form of wavelet matrix transform for effective solutions of electromagnetic problems by Wagner and Chew [19] and the authors [20]. The wavelet transform can adaptively fit itself to various level scales by distributing the localized functions near the discontinuities and the more spatially diffused ones over the smooth expanses of the model. Therefore, the use of the WTM can result in a sparse moment matrix.

In this work, a hybrid method combining the MoM, the FEM and the WTM is proposed for efficient solutions of EM problems with arbitrarily inhomogeneous materials. The equivalence principle is used to divided the original problem into the interior and exterior problems which are solved by the FEM and the MoM, respectively. The two problems are coupled together along the shared boundary to reproduce the original problem. As mentioned above, the FEM results in a sparse matrix, but the traditional MoM always results in a fully populated matrix. To overcome the difficulty solving a full matrix equation, the hybrid method uses the WTM in the conventional MoM. Instead of using wavelet expansion method, a more effective wavelet matrix transform method is employed here. An effective wavelet transform matrix is well constructed by the method in [20]. Using the constructed wavelet transform matrix, one can transform the dense matrices into sparse ones, and furthermore, one can overcome the "edge effect" and avoid a great number of numerical integral operations inevitably existing in the basis expansion methods.

Uniting the advantages of the EEM, the MoM and the WTM, the hybrid technique is able to effectively handle unbounded problems in which complex inhomogeneities are present. For larger-size electromagnetic problems, the proposed technique is more effective compared

with the conventional approaches. Numerical results are presented to show the effectiveness, versatility and validity of the method.

2. FORMULATION

Consider the scattering from an arbitrarily shaped, inhomogeneous, and lossy dielectric body under the illumination of an incident field $(\mathbf{E}^i, \mathbf{H}^i)$ as shown in Fig. 1. Using the equivalence principle, the original problem can be divided into two equivalent problems, i.e., an exterior problem and an interior problem, as shown in Fig. 2. The scattering body bounded by a fictitious surface S and the interior region is characterized by a pair of complex functions $(\epsilon(\mathbf{r}), \mu(\mathbf{r}))$ where $\epsilon(\mathbf{r})$ and $\mu(\mathbf{r})$ denote the permittivity and the permeability, respectively, and $\mathbf{r}$ is the radial position vector in the general 3-D coordinate system. The region outside the surface S is the exterior region which is assumed to be characterized by (ϵ_0, μ_0) where ϵ_0 and μ_0 are the permittivity and the permeability in in free space without loss of generality. The aim is to determine the electromagnetic fields everywhere in the space.

For the exterior problem, the scattering body is replaced with air and the equivalent boundary electric or magnetic currents $\mathbf{J}$ is introduced on the boundary, shown in Fig. 2(a). The total electric field $\mathbf{E}^{ex}$ and magnetic field $\mathbf{H}^{ex}$ in the exterior region are determined by

$$\mathbf{E}^{ex} = \mathbf{E}^i + \mathbf{E}^s(\mathbf{J}), \qquad \mathbf{H}^{ex} = \mathbf{H}^i + \mathbf{H}^s(\mathbf{J}) \tag{1}$$

where the superscripts i and s mean the incident field and scattering field, respectively.

For the interior problem, as shown in Fig. 2(b), the fields inside the boundary S are determined by the tangential electric or magnetic field $\mathbf{F}$ on the boundary S, which means that the interior fields are the functions with variable $\mathbf{F}$, i.e.,

$$\mathbf{E}^{in} = \mathbf{E}^{in}(\mathbf{F}), \qquad \mathbf{H}^{in} = \mathbf{H}^{in}(\mathbf{F}). \tag{2}$$

The two problems are coupled by enforcing the continuity conditions of tangential electric and magnetic fields on the boundary S as follows:

$$\hat{n} \times \mathbf{E}^{ex} = \hat{n} \times \mathbf{E}^{in}, \quad \hat{n} \times \mathbf{H}^{ex} = \hat{n} \times \mathbf{H}^{in} \quad \text{on } S. \tag{3}$$

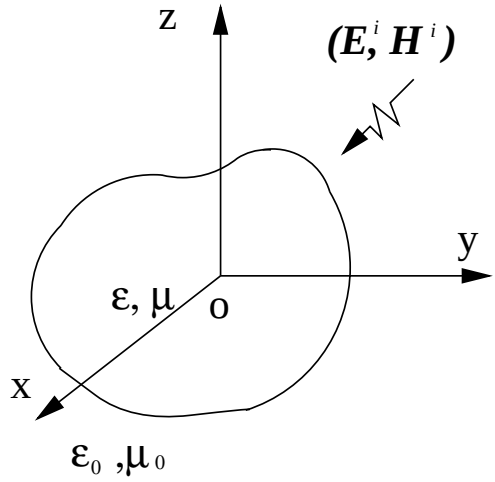

Figure 1. Scattering from a dielectric body in free space.

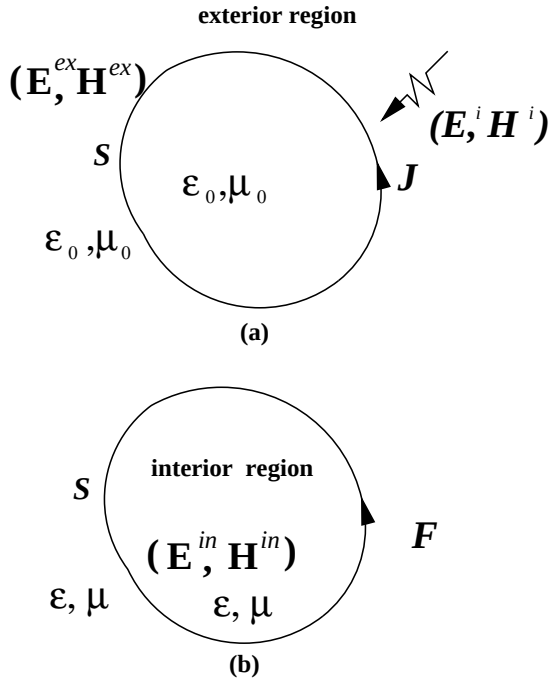

Figure 2. The equivalence of the original problem. (a) Equivalent exterior problem. (b) Equivalent interior problem.

where $\hat{n}$ denotes the outward directed unit normal vector to the surface of the boundary S. Substituting (1) and (2) into (3), we obtain

$$\begin{aligned} \hat{n} \times [\mathbf{E}^{in}(\mathbf{F}) - \mathbf{E}^{s}(\mathbf{J})] &= \hat{n} \times \mathbf{E}^{i} \quad \text{on } S, \\ \hat{n} \times [\mathbf{H}^{in}(\mathbf{F}) - \mathbf{H}^{s}(\mathbf{J})] &= \hat{n} \times \mathbf{H}^{i} \quad \text{on } S. \end{aligned} \tag{4}$$

Equations in (4), together with the Maxwell's equations, are sufficient to determine the equivalent current $\mathbf{J}$ and the equivalent tangential electric or magnetic field $\mathbf{F}$.

A. The MoM for the Exterior Problem

Equations in (4) can be reduced to weak-form matrix equations by the MoM [1]. The unknown $\mathbf{J}$ and $\mathbf{F}$ are approximated by

$$\mathbf{J} = \sum_{j=1}^{M_s} J_j \mathbf{\Psi}_j, \qquad \mathbf{F} = \sum_{j=1}^{M_s} F_j \mathbf{\Psi}_j \tag{5}$$

where $\{\mathbf{\Psi}_j\}$ is a set of chosen expansion functions, M_s is the number of functions chosen, and $\{J_j\}$ and $\{F_j\}$ are two sets of coefficients to be determined. A symmetric product is defined by

$$\langle \mathbf{A}, \mathbf{B} \rangle = \int_s \mathbf{A} \cdot \mathbf{B} ds \tag{6}$$

where $\mathbf{A}$ and $\mathbf{B}$ are two vector functions defined on S. After weighting the equations in (4) with a set of weighting functions $\{\mathbf{W}_j\}$ $(j = 1, 2, 3, ..., M_s)$, the following matrix equation is produced:

$$AX = B \tag{7}$$

where

$$A = \begin{bmatrix} Z^{in} & Z^{ex} \\ Y^{in} & Y^{ex} \end{bmatrix}, \quad X = \begin{bmatrix} F \\ -J \end{bmatrix}, \quad B = \begin{bmatrix} V \\ I \end{bmatrix} \tag{8}$$

and J and F are $M_s \times 1$ vectors with J_j and F_j as their elements, respectively. V and I are $M_s \times 1$ vectors whose ith elements are given by

$$V_i = \langle \mathbf{W}_i, \hat{n} \times \mathbf{E}^{i} \rangle, \qquad I_i = \langle \mathbf{W}_i, \hat{n} \times \mathbf{H}^{i} \rangle. \tag{9}$$

Z^{ex}, Z^{in}, Y^{ex} and Y^{in} are $M_s \times M_s$ matrices whose ij-th elements are respectively given as follows:

$$Z_{ij}^{ex} = \langle \mathbf{W}_i, \hat{n} \times \mathbf{E}^s(J_j) \rangle \qquad \text{on } S, \tag{10}$$

$$Z_{ij}^{in} = \langle \mathbf{W}_i, \hat{n} \times \mathbf{E}^{in}(F_j) \rangle \qquad \text{on } S, \tag{11}$$

$$Y_{ij}^{ex} = \langle \mathbf{W}_i, \hat{n} \times \mathbf{H}^s(J_j) \rangle \qquad \text{on } S, \tag{12}$$

$$Y_{ij}^{in} = \langle \mathbf{W}_i, \hat{n} \times \mathbf{H}^{in}(F_j) \rangle \qquad \text{on } S. \tag{13}$$

Any combination of current-tangential field can be chosen as $(\mathbf{J}, \mathbf{F})$. For two-dimensional EM problems, it is more convenient to choose $\mathbf{J}$ and $\mathbf{F}$ to stand for the equivalent electric current and the equivalent tangential magnetic field for the TM (transverse magnetic) case, and the equivalent magnetic current and the equivalent tangential electric field for the TE (transverse electric) case, respectively. For three-dimensional EM problems, however, it is not clear which combination is a preferred choice. Therefore, one can establish several different formulations; however, the computational complexity will remain the same. In this paper, we choose ($\mathbf{J}$ and $\mathbf{F}$) to be the equivalent electric current and the equivalent tangential magnetic field without loss of generality. The formulations for other kinds of combinations can be easily derived in the similar procedure. The scattering electric field produced by the electric current of unit strength, $\mathbf{\Psi}_j$, in the exterior region can be determined by [5]

$$\begin{aligned} \mathbf{E}^s(\mathbf{\Psi}_j) = & -ik_0 Z_0 \oint_S \mathbf{\Psi}_j G_0(\mathbf{r}, \mathbf{r}') dS' \\ & -i\frac{Z_0}{k_0} \oint_S \nabla' \cdot \mathbf{\Psi}_j \nabla G_0(\mathbf{r}, \mathbf{r}') dS' \end{aligned} \tag{14}$$

where $G_0(\mathbf{r}, \mathbf{r}')$, k_0 and Z_0 are the Green's function, the wave number and the intrinsic impedance in the free space, respectively, and a harmonic time dependence $e^{i\omega t}$ is assumed and suppressed throughout the paper. The scattering magnetic field can be obtained from the Maxwell's equations. In particular, if the observation point $\mathbf{r}$ limits to the surface S of the boundary, the tangential magnetic field takes the following form [21]:

$$\begin{aligned} \hat{n} \times \mathbf{H}^s(\mathbf{\Psi}_j) &= \lim_{\mathbf{r} \to S} \frac{\hat{n} \times \nabla \times \mathbf{E}^s(\mathbf{\Psi}_j)}{-i\omega\mu_0} \\ &= \mathbf{\Psi}_j/2 + \hat{n} \times \oint_S \mathbf{\Psi}_j \times \nabla' G_0(\mathbf{r}, \mathbf{r}') dS' \end{aligned} \tag{15}$$

where $\mathbf{r}$ approaches S from the exterior region side of S. Equations (14) and (15) may be substituted into (10) and (12) to evaluate Z_{ij}^{ex} and Y_{ij}^{ex}. Once the weighting functions $\{\mathbf{W}_i\}$ and the basis functions $\{\mathbf{\Psi}_i\}$ are chosen and the incident fields $(\mathbf{E}^i, \mathbf{H}^i)$ are given, V_i and I_i in (9) can be evaluated. The evaluation of $\hat{n} \times \mathbf{H}^{in}(F_j)$ in (13) is easy since $\hat{n} \times \mathbf{H}^{in}(F_j)$ on S is simply $\mathbf{\Psi}$ itself the tangential magnetic field. The evaluation of (11) which requires knowledge of $\mathbf{E}^{in}(F_j)$ will resort to the FEM in the Section 2-C.

B. The WTM for Sparse Moment Matrices

As mentioned above, using traditional basis and weighting functions the MoM always generates a full matrix. One can see from (10), (12) and (13) that both submatrices Y^{ex} and Z^{ex} are full matrices. However, Y^{in} is a diagonal matrix since the electric (or magnetic) current expansion function resides only on a single segment of the contour. Therefore, the inversion of Y^{in} is trivial. we carry out a simple matrix manipulation of (7) to reduce it into an only $M_s \times M_s$ matrix equation as follows:

$$A_1 J = B_1, \tag{16}$$

where $A_1 = Z^{in}{Y^{in}}^{-1}Y^{ex} - Z^{ex}$ and $B_1 = V - Z^{in}{Y^{in}}^{-1}I$. Once J is solved, F can be obtained by

$$F = {Y^{in}}^{-1}(I + Y^{ex}J). \tag{17}$$

Since the property of A_1 in (16) is completely determined by both Z^{ex} and Y^{ex}, A_1 is a full matrix. We employ the wavelet transform method (WTM) to overcome the difficulty in solving a dense matrix equation. One can directly use wavelets as the basis and weighting functions in the MoM. However, a difficulty is encountered that the wavelet expansion for a given function of finite support requires that some of the wavelet functions reside outside that support, thus resulting in the so-called "edge effect". Since the equivalent current on the fictitious boundary under analysis is defined on the finite surface, the wavelets in the wavelet expansion of the equivalent current are truncated at the boundary points. Hence, non-physical solutions at the boundary points are produced. Furthermore, a great number of wavelet integrations are required to evaluate both Z^{ex} and Y^{ex}. Since few wavelets can be solved in closed form, it is an exhaustive task to directly carry out such kinds of wavelet integrations.

In this work, an effective wavelet matrix transform method is employed. The point-matching method is used in the MoM to rapidly produce both Z^{ex} and Y^{ex} matrices. A general wavelet transform matrix is well constructed for our problem according to the method in [20]. Here non-orthonormal cardinal spline wavelets (NCSW) [14, 15] are used. Note that the singularities of the integral kernels in (10) and (12) are determined by the basic Green's function G_0 or the normal derivative of basic Green's function G_0, and A_1 consists of the linear combination of Z^{ex} and Y^{ex}. Therefore, in order to obtain a satisfactory compression rate to A_1 and a rapidly convergent solution by the wavelet transform for the considered problem, the number of vanishing moments of the wavelets is chosen to be 8 as recommended in [20].

Let $\tilde{U}$ be the $M_s \times M_s$ wavelet basis matrix constructed by the method in [20]. Applying the constructed wavelet matrix $\tilde{U}$ to transform (16), one can obtain a completely sparse matrix equation as follows:

$$A'J' = B' \tag{18}$$

where $A' = \tilde{U}A_1\tilde{U}^T$, $J' = (\tilde{U}^T)^{-1}J$ and $B' = \tilde{U}B_1$. Note that A' in (18) is a non-similarity transform due to $\tilde{U}\tilde{U}^T \neq I$. Furthermore, A' is a sparse matrix for a given threshold value. Therefore, J' can be efficiently solved by a sparse solver. Once J' is solved, one can use the reconstruction algorithm of the wavelet transform to solve J by $J = \tilde{U}^T J'$. Finally, F can be obtained from (17).

C. The FEM for the Interior Problem

As seen above, we have to evaluate $\mathbf{E}^{in}(F_j)$ before solving (7). Since $\mathbf{F}$ is used to denote the equivalent tangential magnetic field on S, $\mathbf{E}^{in}(F_j)$ stands for the electric field due to the equivalent tangential magnetic field $\mathbf{F}_j = F_j\mathbf{\Psi}_j$ defined everywhere on S. Hence, to find $\mathbf{E}^{in}(F_j)$ is to solve a pure boundary value problem. A traditional method to solve the fields in the interior region is to consider the functional [5]

$$\begin{aligned} F(\mathbf{E}^{in}) = \frac{1}{2}\iiint_V \{\frac{1}{\mu_r}(\nabla \times \mathbf{E}^{in}) \cdot (\nabla \times \mathbf{E}^{in}) \\ - k_0^2\epsilon_r \mathbf{E}^{in} \cdot \mathbf{E}^{in}\} dV - ik_0 Z_0 \oint_S \mathbf{E}^{in} \cdot \mathbf{F} dS \end{aligned} \tag{19}$$

via enforcing $\delta F(\mathbf{E}^{in}) = 0$ where δ means the variation of order one. To discretize the functional F, we subdivide the volume V into small

volume elements and with each element we expand the electric field as follows:

$$\mathbf{E}^e = \sum_{j=1}^{n} E_j^e \mathbf{N}_j^e \tag{20}$$

where n is the number of expansion terms, $\{E_j^e\}$ denote the unknown expansion coefficients, and $\{\mathbf{N}_j^e\}$ stand for the chosen vector basis functions for the e-th element. Within each surface patch, the surface field can be expanded as

$$\hat{z} \times \mathbf{E}^s = \sum_{j=1}^{n_s} E_j^s \mathbf{S}_j^s \tag{21}$$

where dominantly $\mathbf{S}_j^s = \hat{z} \times \mathbf{N}_j^s$ on S. Taking the partial derivative of $F(\mathbf{E}^{in})$ with respect to each E_j and setting the resultant expression to zero, we obtain the finite element matrix equation

$$KE^{in} = F_0 \tag{22}$$

where K is a square, sparse, banded, and nonsingular $M \times M$ matrix, and E^{in} and F_0 are $M \times 1$ column vectors where M denotes the total number of the nodes. The detailed form of K and F_0 can be found in [5]. $\mathbf{E}^{in}(F_j)$ can be obtained by evaluating the right-hand side of (22) by replacing $\mathbf{F}$ in (19) with tangential magnetic field of unit strength, i.e., $\mathbf{\Psi}$ and solving the matrix equation (22). M_s such solutions are required, but the matrix K needs to be carried out LU decomposition only once. Finally, substitute the M_s resultant $\mathbf{E}^{in}(F_j)$ ($j = 1, 2, 3, ..., M_s$) into (11) to evaluate Z_{ij}^{in}. Equation (7) can be solved by the WTM to obtain F and J. Hence, the electromagnetic fields at any point in the space can be obtained by (1), (2) and (5); (14) and (15) for the exterior solution, and (22) for the interior solution.

3. NUMERICAL RESULTS

Although the formulation given above is general, numerical results are presented only for the two-dimensional scattering problem.

In the two-dimensional case, the surface boundary S becomes a contour Γ in xy-plane. The surface equivalent currents become line currents. The incident field is assumed to be either a TM (E_z-polarization) or a TE (H_z-polarization) plane wave given by

$$\mathbf{E}^i = \hat{z} E_z = \hat{z} \exp[ik_0(x \cos \varphi_i + y \sin \varphi_i)] \tag{23}$$

for TM case, and

$$\mathbf{H}^i = \hat{z}H_z = \hat{z}\frac{1}{Z_0}\exp[ik_0(x\cos\varphi_i + y\sin\varphi_i)] \tag{24}$$

for TE case. Thus, the equivalent electric or magnetic current sources will also be z-directed.

Note that TE and TM modes are dual to each other. That is, all the relative submatrices for the TM case can be obtained directly from those for the TE case.

For our problem, the interested parameter is the radar cross section (RCS) which is defined by

$$\sigma = \lim_{r\to\infty}(2\pi r\frac{|\mathbf{H}_s|^2}{|\mathbf{H}^i|^2}) \tag{25}$$

for the TE case, and

$$\sigma = \lim_{r\to\infty}(2\pi r\frac{|\mathbf{E}_s|^2}{|\mathbf{E}^i|^2}) \tag{26}$$

for the TM case.

It should be emphasized that to minimize the computation, the fictitious boundary Γ should be chosen to make the interior region as small as possible. Furthermore, if the chosen Γ makes the integrals in (10) and (12) convolutional, one can only need to evaluate one row or column to form the complete matrices Z^{ex} and Y^{ex}, thus reducing the filling time significantly. For many practical EM problems, such kinds of choices are suitable and feasible. Furthermore, because of the localized properties of multiresolution analysis the moment matrices from the WTM are almost diagonal if the fictitious boundary is chosen as smooth as possible.

Several examples involving scattering from homogeneous as well as inhomogeneous circular dielectric cylinders are presented. For the proposed EM problems, the best fictitious boundary Γ is the outer natural boundary of the dielectric cylinder. First, consider the scattering from a homogeneous dielectric cylinder. We discretize the interior region into small elements by dividing the radius direction into 12 equithickness layers and the polar angle direction into 128 equal segments, i.e., $M_s = 128$. Fig. 3 shows the 3-D logarithmic plots of the normalized magnitudes of the entries in matrices A by the MoM/FEM

and A_1 by this technique for TM case. It can be observed from Fig. 3 that if a threshold of 10^{-5} is set, the matrix A_1 from this technique gives a sparse matrix with only 4.68% of the total elements (16384) left, while the matrix A from the conventional MoM/FEM turns out a dense matrix.

In Fig. 4, more details are given to show the sparse distributions of the elements in matrix A_1 with a threshold of $\tau/m = 10^{-5}$ or $\tau/m = 10^{-4.5}$ for both TM and TE cases, respectively. Here, m stands for the largest magnitude of elements in A_1 and R is defined as the populated rate (the ratio of the number of remaining nonzero elements after thresholding to the total number of elements in A_1). It can be observed from Fig. 4 that almost all the off-diagonal elements in the transformed matrix A_1 are equal to zeros. We will see later that the approximate solutions from the equation (16) are of good accuracies even with so sparse matrices A_1 . The advantage of a sparse matrix over a dense matrix is important since sparse matrix solvers are much faster and need much smaller storage space than general dense matrix solvers. The advantage become more profound as a large matrix system is involved.

Fig. 5 shows the RCS of the circular dielectric cylinder under TE or TM plane wave incidence. Let the incident angle $\varphi_i = \pi$, the radius $a = 0.3\lambda$, the working frequency $f = 300\,\mathrm{MHz}$, $\epsilon_r = 4.0$ and $\mu_r = 1.0$. The classical eigenfunction solutions are obtained by summing the Fourier series up to 30 terms. The results by this technique are solved by setting the threshold values $\tau/m = 10^{-4.5}$ with $R = 1.84\%$ and $R = 2.43\%$ for TM and TE cases, respectively. Even with so sparse matrices the results by this technique show good agreement to the accurate solutions.

In Fig. 6, the proposed technique is used to compute the RCS of the circular dielectric shell and the results are compared with the ones by the MoM/FEM (i.e., $R = 100\%$) under TM incident waves. Good approximate solutions can be obtained by this technique even with so a low populated rate ($R = 3.89\%$ and $R = 3.41\%$ for lossless and lossy cases, respectively).

The proposed approach can be also used to analyze scattering from cylinders with arbitrary inhomogeneities. To demonstrate this we analyze scattering from a four-layered dielectric cylinder with circular cross section. Results compared with the ones by the MoM/FEM for the TM scattering are shown in Fig. 7. Even with so sparse matrix

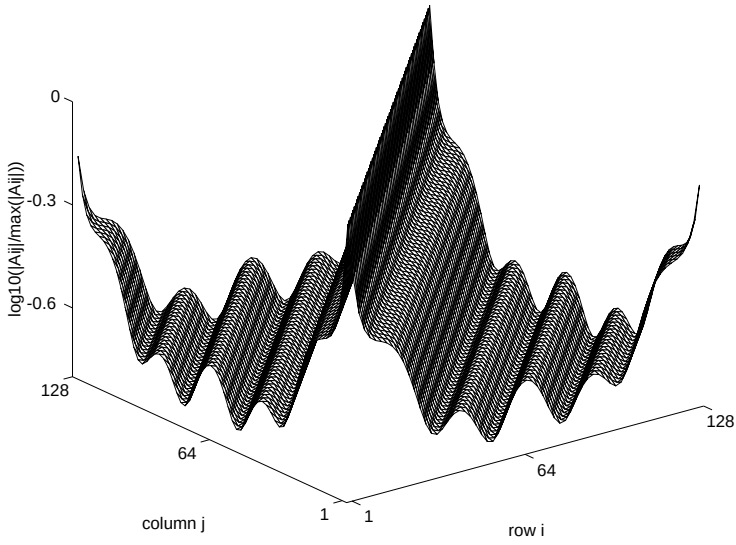

(a)

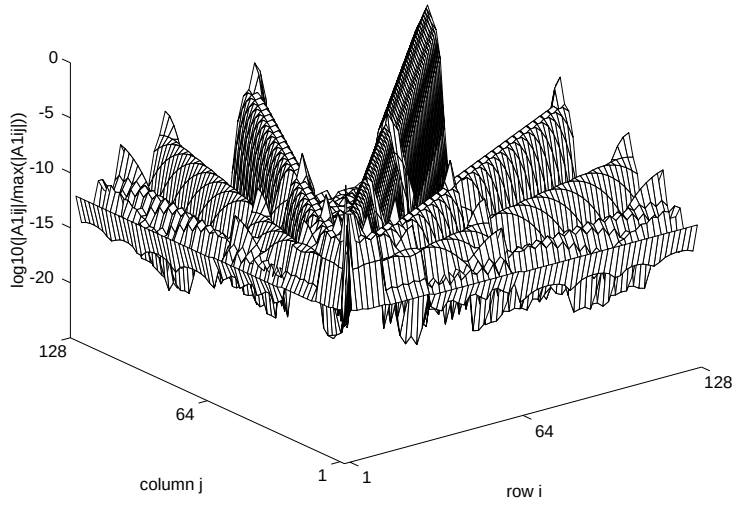

(b)

Figure 3. 3-D logarithmic plots of the magnitudes of the entries in the moment matrices for a homogeneous dielectric cylinder under TM excitation. (a) A by the MoM/FEM. (b) A_1 by the MoM/FEM/WTM.

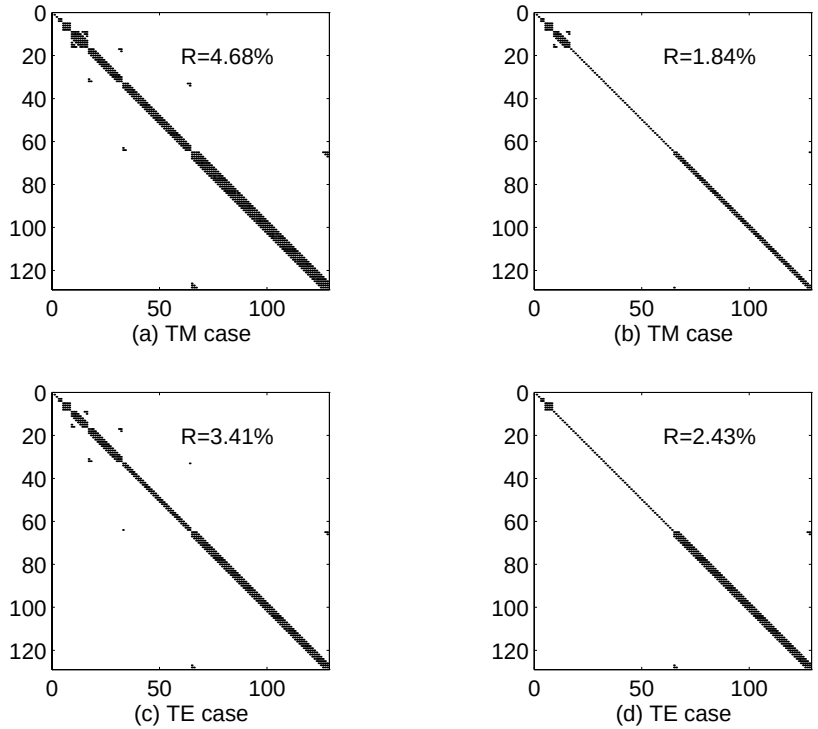

Figure 4. The remaining nonzero elements of A_1 after setting to zero each element whose magnitude is smaller than a selected threshold τ. (a) and (b) for TM case and (c) and (d) for TE case. Also indicated for each threshold is the population rate R to which a threshold $\tau/m = 10^{-5}$ for (a) and (c), or $\tau/m = 10^{-4.5}$ for (b) and (d) is related. m is the largest magnitude of elements in A_1.

equations the solutions by this technique show good accuracies.

It is deserved to be emphasized that the proposed hybrid method can effectively handle other kinds of complex and larger EM problems which involve boundaries with arbitrary shapes and scattering bodies with arbitrary inhomogeneities because of the versatility of the WTM and the FEM. It, of course, will result in less sparse WTM matrices than the ones in Fig. 4, but a high compression rate of the WTM matrices can still be obtained. For a large boundary problem, the effectiveness of the proposed hybrid method is outstanding compared with the traditional methods which face with solving a large dense matrix equation.

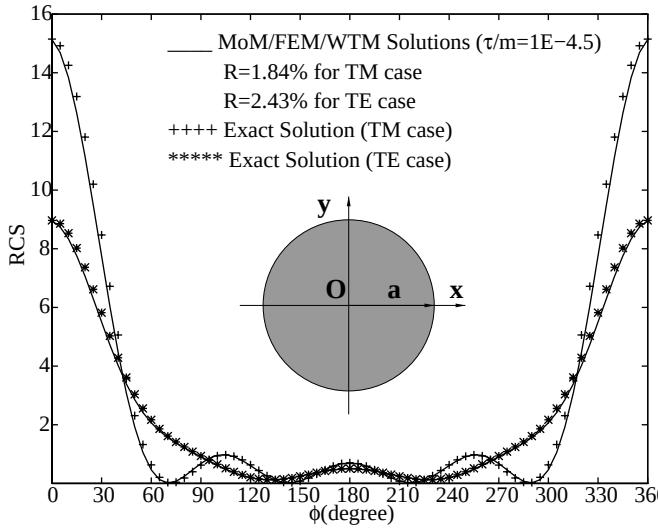

Figure 5. RCS of a circular dielectric cylinder ($a = 0.3\lambda$, $\sigma = 0.0$, $\epsilon_r = 4.0$, $\mu_r = 1.0$, $f = 300MHz$, $\varphi_i = \pi$) under TE or TM plane wave incidence.

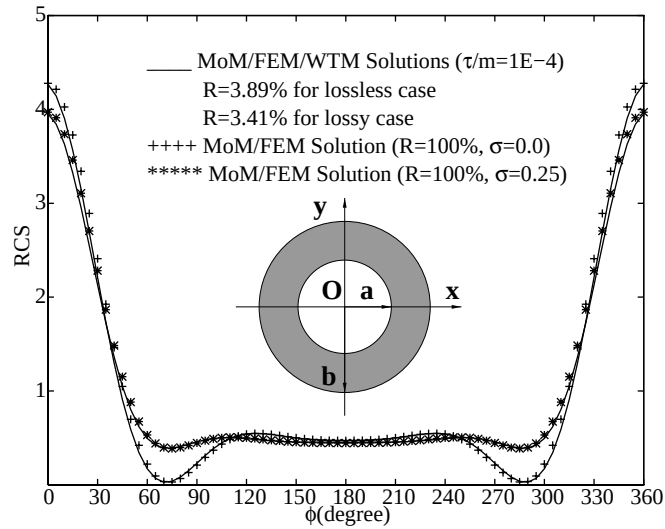

Figure 6. RCSs of a circular dielectric shell ($a = 0.25\lambda$, $b = 0.30\lambda$, $\epsilon_r = 4.0$, $\mu_r = 1.0$, $f = 300MHz$, $\varphi_i = \pi$) with lossless ($\sigma = 0.0$) or lossy ($\sigma = 0.25$) material under TM plane wave incidence.

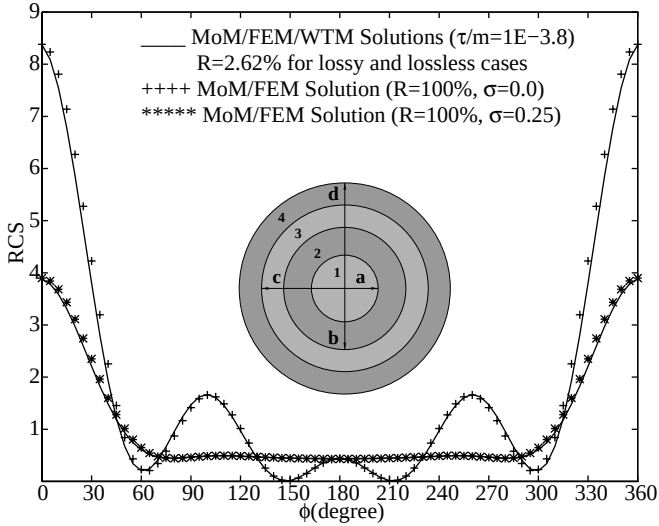

Figure 7. RCSs of a four-layered circular inhomogeneous cylinder ($a = 0.15\lambda$, $b = 0.20\lambda$, $c = 0.25\lambda$, $d = 0.30\lambda$, $\epsilon_{r1} = 8.0$ (innermost layer), $\epsilon_{r2} = 6.0$, $\epsilon_{r3} = 4.0$, $\epsilon_{r4} = 2.0$ (outmost layer), $\mu_r = 1.0$, $f = 300MHz$, $\varphi_i = \pi$, and σ is the same in all layers) under TM plane wave incidence.

4. CONCLUSIONS

In this paper, the hybrid MoM/FEM/WTM method has been proposed. Uniting the advantages of the MoM, the FEM, and the WTM, the hybrid method employs the MoM and the WTM to handle unbounded problems effectively, and the FEM to efficiently solve boundary value problems where arbitrary inhomogeneities are present.

Since the interior and exterior problems are coupled only on the shared fictitious boundary, the finite element matrix needs to be computed and carried out by LU decomposition only once. Hence, little extra computations are needed if the incident waves change. Furthermore, the use of the point-matching method and the proposed WTM avoids a great number of integral operations and always results in a sparse moment matrix for the exterior problems. Meanwhile, the so-called "edge effect" has been overcome, thus improving the solution accuracies significantly.

The versatility of the proposed method is dominant because on one hand, the radiation properties are naturally included in the MoM and

the scattering problems involving inhomogeneous medium are easily and systematically handled by the FEM, and on the other hand, one can obtain solutions of arbitrary accuracy to the practical EM problems through choosing the proper fine finite element mesh in the FEM and the suitable threshold value in the WTM. The validity and accuracy of the solutions by the proposed hybrid method are confirmed by the exact analytical series solutions in the two-dimensional environment. There is no restriction on the shape or inhomogeneity of the scatterer and absorber to be solved because of the versatilities of the FEM and the WTM. Future efforts will be directed to the problems involving perfect conductors and arbitrarily shaped three-dimensional problems.

REFERENCES

1. Harrington, R. F., *Field Computation by Moment Method,* New York: Macmillan, 1968.
2. Morita, N., "Surface integral representation for electromagnetic scattering from dielectric cylinders," *IEEE Trans. Antennas Propag.,* Vol. 26, 261–266, Mar. 1978.
3. Richmond, J. H., "Scattering by a dielectric cylinder of arbitrary cross section shape," *IEEE Trans. Antennas Propag.,* Vol. 13, 334–341, May 1965.
4. Mei, K. K., "Unimoment method of solving antenna and scattering problems," *IEEE Trans. Antennas Propag.,* Vol. 22, 760–766, Nov. 1974.
5. Jin, J. M., *The Finite Element Method in Electromagnetics,* New York: Wiley, 1993.
6. Harrington, R. F., *Time Harmonic Electromagnetic Fields,* McGraw-Hill, 1961.
7. Jin, J. M., J. L. Volakis, and J. D. Collins, "A finite element-boundary integral method for scattering and radiation by two- and three-dimensional structures," *IEEE Antennas and Propagation Magazine,* Vol. 33, No. 3, 22–32, June 1991.
8. Collins, J. D., J. M. Jin, and J. L. Volakis, "A combined finite element-boundary element formulation for solution of two-dimensional problems via CGFFT," *Electromagnetics,* Vol. 10, No. 4, 423–437, 1990.
9. Jin, J. M. and V. V. Liepa, "Application of hybrid finite element method to electromagnetic scattering from coated cylinders," *IEEE Trans. Antennas Propag.,* Vol. 36, 50–54, Jan. 1988.

10. Yuan, X., D. R. Lynch, and J. W. Strohbehn, "Coupling of finite element and moment methods for electromagnetic scattering from inhomogeneous objects," *IEEE Trans. Antennas Propag.* Vol. 38, No. 3, 386–393, March 1990.
11. Jankovic, Dj., M. S. LaBelle, D. C. Chang, J. M. Dunn, and R. C. Booton, "A hybrid method for the solution of scattering from inhomogeneous dielectric cylinders of arbitrary shape," *IEEE Trans. Antennas Propag.* Vol. 42, No. 9, 1215–1222, Sept. 1994.
12. Alpert, B., G. Beylkin, R. Coifman, and V. Rokhlin, "Wavelet-like bases for the fast solution of second-kind integral equations," *SIAM J. Sci. Comput.,* Vol. 14, No. 1, 159–184, Jan. 1993.
13. Daubechies, I., *Ten Lectures on Wavelets,* Philadelphia, PA: Society for Industrial and Applied Mathematics, 1992.
14. Chui, C. K., *An Introduction to Wavelets,* Boston MA: Academic Press, 1992.
15. Chui, C. K., and J. Wang, "On compactly supported spline wavelets and a duality principle," *Trans. Amer. Math. Soc.,* Vol. 330, 903–915, 1992.
16. Steinberg, B. Z., and Y. Leviatan, "On the use of wavelet expansions in the method of moments," *IEEE Trans. Antennas Propag.,* Vol. 41, No. 5, 610–619, May 1993.
17. Sabetfakhri, K., and L. P. B. Katehi, "Analysis of integrated millimeter-wave and submillimeter-wave waveguides using orthonormal wavelet expansions," *IEEE Trans. Microwave Theory Tech.,* Vol. MTT-42, No. 12, 2412–2422, Dec. 1994.
18. Wang, G., and G. Pan, "Full wave analysis of microstrip floating line structures by wavelet expansion method," *IEEE Trans. Microwave Theory Tech.,* Vol. MTT-43, No. 1, 131–142, Jan. 1995.
19. Wagner, R. L., and W. C. Chew, "A study of wavelets for the solution of electromagnetic integral equations," *IEEE Trans. Antennas Propag.,* Vol. 43, No. 8, 802–810, Aug. 1995.
20. Xiang, Z., and Y. Lu, "An effective wavelet matrix transform approach for efficient solution of electromagnetic integral equations," *IEEE Trans. Antennas Propag.,* Vol. 45, No. 1, 1205–1213, August 1997.
21. Van Bladel, J., *Electromagnetic Fields,* New York: McGraw-Hill, 1968.